

Service Restoration in Modern Distribution Systems Addressing Grid-Connected and Islanded Operations

W. R. Faria, E. O. P. Carvalho, L. B. Dantas, C. D. Maciel, L. F. C. Alberto, J. B. A. London Junior and B. R. Pereira Junior

Abstract—In modern Distribution Systems (DSs), multiple decentralized generators can be connected to the network and, in some scenarios, can operate isolated from the substation. The island operation affects the Service Restoration (SR) process and may benefit the Distribution Companies (DICOs). However, most of the studies involving SR take into account only the system's static behavior, ignoring the transient characteristics. While these studies have been validated for decades on classic passive DSs, they cannot be extended for SR with load insertion into islands. This paper studies the dynamic aspects of the SR process, verifying the protective devices' performance due to the island's formation and operation, and loads reconnection through Distributed Generators (DGs). Based on the test results for a 405-bus DS, the paper points out the possibility of infeasible SR plans due to disregarding the transient behavior of DGs. The paper also proposes a novel set of constraints that aggregates practical dynamic and static aspects for the SR problem. Finally, a computationally efficient Multi-Objective Evolutionary Algorithm (MOEA) based on subpopulation tables is employed to solve the SR problem considering the newly proposed constraints.

Keywords—Frequency protection, intentional islanding, power distribution protection, transient frequency.

I. INTRODUCTION

Outages caused by permanent faults or damaged equipment can cause large out-of-service (OFS) areas in a Distribution System (DS). Their effects are minimized by means of system reconfiguration, which is the process of altering the topological structure of the DS by opening sectionalizing (normally closed (NC)) switches, and closing tie (normally open (NO)) switches. Finding the switches to be maneuver is not an easy task, and determining these is the purpose of the well-known Service Restoration (SR) problem.

The SR problem is one of the most relevant topics related to the efficient operation of a DS [1], [2] and emerges after the area of the fault has been identified and isolated. A solution, named Service Restoration Plan (SRP), is obtained by determining the minimum number of switching operations that result in a configuration with a minimal number of OFS areas. Additionally, a SRP must maintain the radial structure and comply with the operational constraints (bounds for node voltage, network loading, and substation loading) of the network. Amongst the characteristics that make the SR a difficult task, one can mention that it is a complex combinatorial optimization problem involving multiple non-linear constraints and objective functions. Moreover, a SRP should be quickly found to ensure customer's satisfaction and avoid penalizing the Distribution Companies (DICOs) [2], [3].

The increase of Distributed Generator (DG) penetration changes the way of dealing with most problems regarding the planning and operation of DSs, including the SR problem. The presence of DGs in DSs raises the need to reassess the traditional methodologies for

planning and operating DSs, or develop new ones. In the context of the SR problem, DGs can improve the voltage profile, relieve the power flowing through components of the grid, and enable the power supply during outages as a result of island operation. These improvements collaborate with the interests of DISCOs in turning the DS into a resilient system, *i.e.*, a system capable of absorbing the impacts caused by contingencies without losing its operating capacity [4]. In this context, the IEEE Standard 1547 [5] suggests and regulates the application of intentional islanding, fed by DGs, in OFS areas during outages. Besides the opportunities previously highlighted, the presence of DG in DS also presents challenges for developing SR methodologies, particularly when considering the possibility of intentional islands. Most of the difficulties are related to the fact that, even during the island operation, the DGs must guarantee that their islands operate within acceptable parameters, including frequency, voltage, and equipment ratings [6].

Although the SR problem has been addressed for a long time, the inclusion of DGs and their island operation into the optimization model became a prominent topic only in the past few years [7], [8]. Most of the existing SR methodologies taking these aspects into account consider only the static constraints of the problem, such as the operational limits of DGs [8], [9]. Omitting the dynamic aspects of the problem, mainly during the island formation and load transfer to islands, can lead to infeasible solutions for practical implementation, since, during these procedures, the local protection of each DG can act due to frequency and voltage fluctuations. The authors of [10] investigated these undesired operations; however, no general equation or methodology to determine thresholds was presented to ensure the island operation is maintained. Thus, it is necessary to propose methods incorporating dynamic aspects in the SR problem's conventional static model to ensure that the solutions are feasible for practical implementation [6]. An investigation of the SR problem involving island operation and regarding the DGs' transient characteristics is presented in [11]. However, this proposal does not provide a constraint for the SR optimization problem to guarantee that the DGs operate correctly; instead, the authors evaluate each solution's feasibility by means of a simulation using GridLab-D.

In this paper, practical dynamic constraints associated with the aspects of island operation regulated in [5] are incorporated into the SR problem by converting differential equations into a set of numerical equivalent algebraic equations. As dynamic constraints cannot be expressed as equality or inequality constraints written in terms of known elementary functions, the proposed incorporation is challenging. In addition to the challenging determination of the dynamic constraints, high-cost computational procedures, such as numerical integration of a large set of differential-algebraic equations, are necessary to verify the compliance of such constraints. This paper proposes an empiric strategy to verify these constraints

This work was supported by CNPq (grants 424489/2018-0 and 308297/2018-0) and COPEL S/A (grant PD2866-0504/2018).

by analyzing the dynamic aspects of the SR process, verifying the protective devices' performance due to the island's formation and operation, and loads re-connection utilizing islanded DGs. The computationally efficient Multi-Objective Evolutionary Algorithm (MOEA) based on subpopulation tables proposed in [9] is employed to solve the SR problem considering the proposed constraints. The effectiveness of the paper proposals are confirmed on tests performed on a 405-bus DS, which is also modeled in ATP-EMTP, along with the protective devices installed in the network.

II. SERVICE RESTORATION PROBLEM

Based on the graph representation of a DS, the SR problem was formulated in [9] as shown in (1).

$$\min \begin{cases} ENS(G) \\ \psi(G) \end{cases} \quad (1)$$

$$s.t. \begin{cases} G \text{ must be a graph forest} \\ \text{Maximum and minimum node-voltage} \\ \text{Conductors' maximum current} \\ \text{Maximum substation loading} \\ \text{DG's steady constraints (active power, reactive} \\ \text{power and power factor within its operation limits)} \end{cases}$$

where G is a radial configuration of a DS represented by a graph forest, $ENS(G)$ is the Energy Not Supplied (ENS) including the time interval necessary to execute the switching operations to obtain the final configuration after the fault isolation, $\psi(G)$ is the number of switching operations necessary to reach topology G from the pre-fault configuration (the number of maneuvers to isolate the faulted areas are included).

Observe that (1) does not present any constraints associated with the dynamic aspects of the SR problem. In the next section, dynamic aspects of the SR problem will be modeled in order to include constraints associated with the dynamic aspects in (1).

To solve the augmented formulation, this paper employs the computationally efficient MOEA in subpopulation tables presented in [3], which is capable of dealing with practical aspects of the SR problem (such as load prioritization, different types of switches, load curtailment and switching sequence determination) in large scale DSs, in an appropriate running time (due to the use of the Node-Depth Encoding and its genetic operators), even considering the presence of DGs.

Noteworthy, the effectiveness of any restoration plan is directly affected by the Distribution Company (DISCO)'s capacity of monitoring or forecasting the power demand at each medium voltage bus of the DS, as these values are at the core of the ENS calculation. In this sense, the utilities must have a tool to estimate (or access) the network's power demand regardless of the presence of DGs to execute an effective restoration plan. Such a tool is even more crucial in this study as the load transferring maneuvers may lead to severe transients if not carefully planned. It is important to stress that the DISCO must not necessarily invest in monitoring equipment; alternatively, investments in demand forecasting or loading estimation can produce similar results.

In this study the SRPs are obtained considering the following set of hypotheses:

- It is assumed that the fault location is known prior to the execution of the MOEA in subpopulation tables; hence, the sector affected by the fault is part of the input data;
- The protection system philosophy and setting are outside the scope of this proposal. It is important to stress that the island formation and its maintenance is the protection system responsibility (the protection systems may or may not employ communication links as both approaches can be found in the literature). We address only the load transferring into already formed islands;
- The DISCO has a tool capable of estimating the network's power demand during the repair time. In this context, the critical power demands (maximum and minimum) within the time-window are used in the SR process.

III. DYNAMIC ANALYSES OF THE SR PROBLEM

A. Distributed Generator Modeling

Nowadays, there are many primary energy sources used in distributed energy production. In this paper, we consider synchronous generators moved by steam turbines used, for example, in cogeneration and small thermal power plants. The suggestion presented in [5] is that every DG, in order to operate connected to the main grid, should be able to operate in a few modes, including constant active power injection, constant reactive power injection, frequency-droop, and volt-var. In this sense, we designed the speed governor and exciter control systems based on the generic scheme for steam turbines [12] and the Direct Current Commutator (DC1C) excitation system model [13], respectively. The governor and exciter are illustrated, respectively, in Figs. 1 and 2.

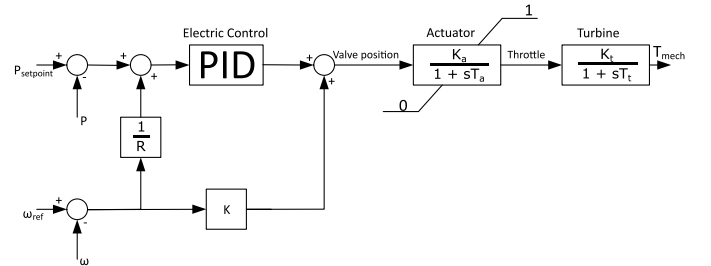


Fig. 1. Speed governor diagram

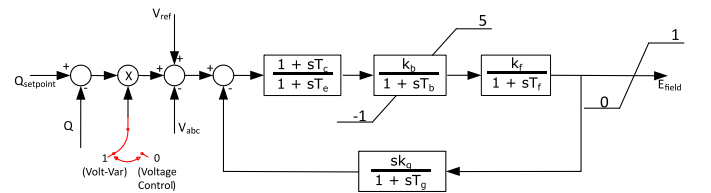


Fig. 2. Direct current commutator exciter diagram

As it can be extracted from the diagrams presented in Figs. 1 and 2, as long as the main grid is capable of providing nominal frequency and voltage, the DG can inject constant active and reactive power. During contingencies, which may cause the DG's island operation, the machine must operate in frequency-droop and/or volt-var mode, depending on which electric variables are affected, as instructed in [5].

B. Constraints Regarding the Islands' Steady-State Operation

Intentional islanding in the service restoration context may improve the system's self-healing capacity and should be performed as soon as possible upon permanent fault events. To attain the most rapid island formation, we consider the presence of an Island Interconnection Device (IID). The IID is a protective device installed at the Point of Common Coupling (PCC) that operates to place a region of the DS in island mode [14]. As soon as the DGs are no longer connected to the main grid, the power balance must be guaranteed by them, and any power mismatch is reflected in voltage or frequency deviations due to droop control. Noteworthy, the island frequency does not return to normal (60 Hz) for as long as the island demand is not close enough to the machine's active power setpoint. The new generator's setpoints are determined externally to the controllers presented in this paper, most likely an Automatic Generation Control (AGC) is employed. Nonetheless, the AGC's response is far slower than the protective devices' [12].

The maintenance of an island is mainly related to the voltage magnitude and the signal's frequency, and so are the thresholds to determine whether or not the DG ceases to energize the island region [5]. In this sense, we consider the DG's local protection to be the association of an under/overfrequency (81UO) and an under/overvoltage (27/59) relays. The additional constraints proposed in this subsection guarantee that the island's frequency and voltage in steady-state, disregarding the AGC's operation, do not drift from the nominal values enough to **cause** the DG's protective devices **to respond**. It is possible to extract from Fig. 1 the frequency-power equilibrium equation shown in (2).

$$\begin{aligned} P_{setpoint} - P_{island} &= \frac{1}{R} \cdot (\omega_{ref} - \omega_{island}) \\ \omega_{island} &= \omega_{ref} - R \cdot (P_{setpoint} - P_{island}) \end{aligned} \quad (2)$$

being $P_{setpoint}$ the DG's active power setpoint, P_{island} the island's active demand. R is the machine's droop, ω_{ref} and ω_{island} are the machine's angular velocity under nominal operation and during the island operation, respectively. Analogously, from the exciter model, we can express the volt-var behavior as presented in (3).

$$\begin{aligned} Q_{setpoint} - Q_{island} &= V_{ref} - V_{island} \\ V_{island} &= V_{ref} - (Q_{setpoint} - Q_{island}) \end{aligned} \quad (3)$$

Adopting $V_{ref} = 1.0$ and the lower and upper voltage limits proposed in [5] (0.88-1.1 p.u.), Q_{island} can neither surpass $Q_{setpoint}$ in more than 0.1 p.u., nor reduce more than 0.12 p.u. It is essential to highlight that the response time of the exciter is narrow and can easily switch from Volt-Var to constant voltage mode. Considering the latter, as long as the DG has enough reactive power capacity to supply the loads, the voltage is kept close to the reference.

Assuming that the DS may have DGs with different droops or the possibility of adopting more cautious frequency limits, the additional constraints can be written in a generic form, as shown in (4).

$$\begin{cases} P_{island} \leq P_{setpoint} + \frac{f_{ref} - \underline{f}}{R} \\ P_{island} \geq P_{setpoint} - \frac{\bar{f} - f_{ref}}{R} \end{cases} \quad (4)$$

wherein \underline{f} and \bar{f} are the frequency lower and upper limits, respectively.

C. Constraints Regarding the Islands' Transients

The island's limits for active and reactive powers presented in section III-B are necessary but may not be sufficient to guarantee the DGs permanent operation and, therefore, the island's maintenance. This scenario may happen because the set of constraints (4) is valid when the accelerating power is zero; nonetheless, there may be no equilibrium between electrical and mechanical torques during the first seconds after the islanding formation. In this scenario, the magnitude and duration of the transient frequency depend on the accelerating power magnitude, the system's inertia (which depends on the parameters of each DG in the island), the speed governor's gains and the loads' behavior [12]. In this context, one must address the frequency's dynamic behavior and ensure that neither magnitude nor duration exceeds the desired limits to guarantee the island's correct operation.

Determining characteristics related to the transient frequency of a generator is a challenging task since its behavior is non-linear and dynamic. In this sense, developing an analytical expression to calculate the critical frequency of a synchronous machine caused by a switching maneuver may not be the best course of action to integrate an optimization tool. Proposing closed form equations that describe the generator's transient behavior as constraints may not be efficient as these would have to be solved using numeric integration, demanding high computational efforts. Another way to address this issue is empirically determining operational limits that ensure critical transient frequencies within convenient boundaries. In this sense, we carried out power mismatches simulations caused by switching maneuvers in ATP-EMTP to determine the most critical transient frequency observed at the terminals of the generator, as illustrated in Fig. 3. In this paper, we employ as lower and upper boundaries the transient frequency limits suggested in [5]: 56.5 Hz and 62 Hz, respectively. This, the minimum and maximum tolerable transient frequency deviations are -3.5 Hz and 2 Hz, respectively. Observe in Fig. 3 that for active power mismatches within the range ξ and ζ the critical frequency deviation values are kept within the limits specified for this study. In this sense, the constraint can be formulated as per se (5).

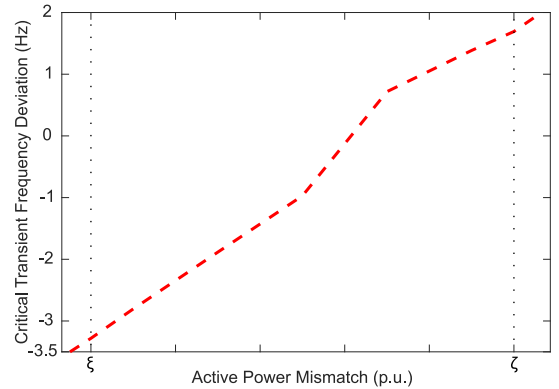


Fig. 3. Illustration of critical active power mismatch determination

$$\begin{cases} \Delta P = P_{current} - P_{new} \leq \zeta \\ \Delta P = P_{current} - P_{new} \geq \xi \end{cases} \quad (5)$$

wherein $P_{current}$ and P_{new} are the DG's instantaneous power injection and the expected demand after a maneuver, respectively. ζ and ξ are, respectively, the maximum and minimum power mismatches for which the transient frequency is within the feasible range. It is imperative to highlight that ΔP is not necessarily associated with the DG's setpoint; instead, ΔP is defined as the difference between the instantaneous power injection and the DG's next demand after a load block is added to or removed from the island.

IV. RESULTS

A. Test System and Data

The tests were carried out on a 405-bus DS composed of three feeders, as illustrated in Fig. 3. There are four DGs scattered throughout the DS, but the analysis performed in this paper focuses on the behavior of DGs 1 and 2, each of them is a 1.5MVA synchronous machine (the capacity of the others DGs is available in [15]). The governor and exciter parameters for both machines are the same, as shown in Table I. The feeders' protection systems were designed as proposed in [14], while the DGs' local protections were created as shown in [10]. The shaded areas in Fig. 4 indicate regions that can be automatically islanded through the IIDs' operations. The data regarding the protective devices' parameters and location, the system's loads, and the branches' impedance are available in [15].

It is important to stress that some events occur before the determination of the SR plan. The complete chain of events is listed below:

- 1) Occurrence of the fault (e.g., short-circuit);
- 2) Substation protection system operates eliminating the contribution of the substation. At the same time the IIDs act putting the DGs in island operation;
- 3) Permanent isolation of the faulted sector;
- 4) Proposition of the restoration plan (this aspect is the focus of this paper)
 - load transfer to other feeders or to health sectors in the same feeder;
 - load transfer into the island regions formed.

Furthermore, the test system was also designed in ATP-EMTP but only to illustrate the feasibility of each maneuver proposed by the optimization method. It is crucial pointing out that the DGs' power injections may vary throughout the day according to the DG owners' interests, energy market contracts, and network constraints, and so does the power system's loading. Thus, the restoration plan for the same fault location may differ depending on the power balance scenario when the fault strikes. In this paper, we present punctual analyses considering specific cases at the edge of the system's stability. Then we create thresholds so that the proposed optimization model for restoration plans are always feasible under both static and transient perspectives.

B. SR without Frequency Constraints

There are three distinct situations transient-wise for restoring loads in a DS with DGs: (1) transferring loads to a feeder without DGs or at least a region electrically far from any generator; (2) transferring loads to a region electrically close to a DG whilst the machine operates connected to the main grid; and (3) transferring loads into an island. To address two of these situations, we present

TABLE I
GOVERNOR AND EXCITER PARAMETERS

Controller	Variable	Value	Controller	Variable	Value
Governor	Droop (R)	0.05	Exciter	T_c	0
	K	0		T_e	0
	K_p (PID)	1		K_b	120
	K_i (PID)	0.1		T_b	0.02
	K_d (PID)	0.3		K_f	1
	K_a	1		T_f	0.8
	T_a	0.1		k_g	0.008
K_t	1	T_g	0.5		
	T_t	1			

the simulation of a fault at bus 78, which is highlighted in Fig. 4. In the sense of complete disregard for the correlation between the power mismatches and frequency/voltage fluctuations, we set the pre-fault injection for both studied DGs as 1.49 MW (0.99 p.u.) and 165 kVAr (0.11 p.u.). It is worth mentioning that the Automatic Islanding Region (AIR) supplied by DG₁ has a 650 kW (0.45 p.u.) demand, while the other AIR's demand is 390 kW (0.26 p.u.). The AIRs' reactive power demands are disregarded, as the DGs keep constant voltage during the island operation. The sequence of maneuvers is presented in Table II. The frequency fluctuations at each DG and at node 1 (substation) due to these topology changes are shown in Fig. 5.

TABLE II
SEQUENCE OF MANEUVERS FOR SCENARIO 1

Scenario	Open*	Close*	ENS**	PNS***
Fault at Bus 78	48-61	-		
	97-98	-		
	95-102	-		
	90-119	-		
	78-79	-	164.26	0.00
	65-66	-		
	103-104	-		
	-	103-104		
	-	70-81		
	-	60-127		
-	99-121			

* Switches between buses.

** Value in kWh calculated for the final topology disregarding the ENS of the faulted sector.

*** (PNS = Power Not Supplied) Value in kW calculated for the final topology disregarding the PNS of the faulted sector.

As shown in Fig. 5 highlighted region, the substation frequency fluctuation during the entire simulation is virtually null. In this sense, the substation frequency is kept within the operational range proposed in [5], even before the fault's clearance. Nonetheless, the substation is disconnected from the grid due to overcurrent. Only after the fault is permanently isolated, the loads are resupplied by the substation. It is important to stress that, when the main grid is re-energized, the substation's injected power goes from 0 to approximately 3 MVA; nevertheless, the frequency variation is essentially zero. This behavior is observed because the substation is connected to the transmission system; therefore, to provoke a frequency deviation in the main feeder, the distribution system re-connection must significantly affect the transmission system's inertia. In this sense, the aggregated inertia of the DS would have to be comparable to the combined inertia of multiple power plants connected to the transmission system. Since that is not the case, the decision to neglect frequency constraints in SR when there are no

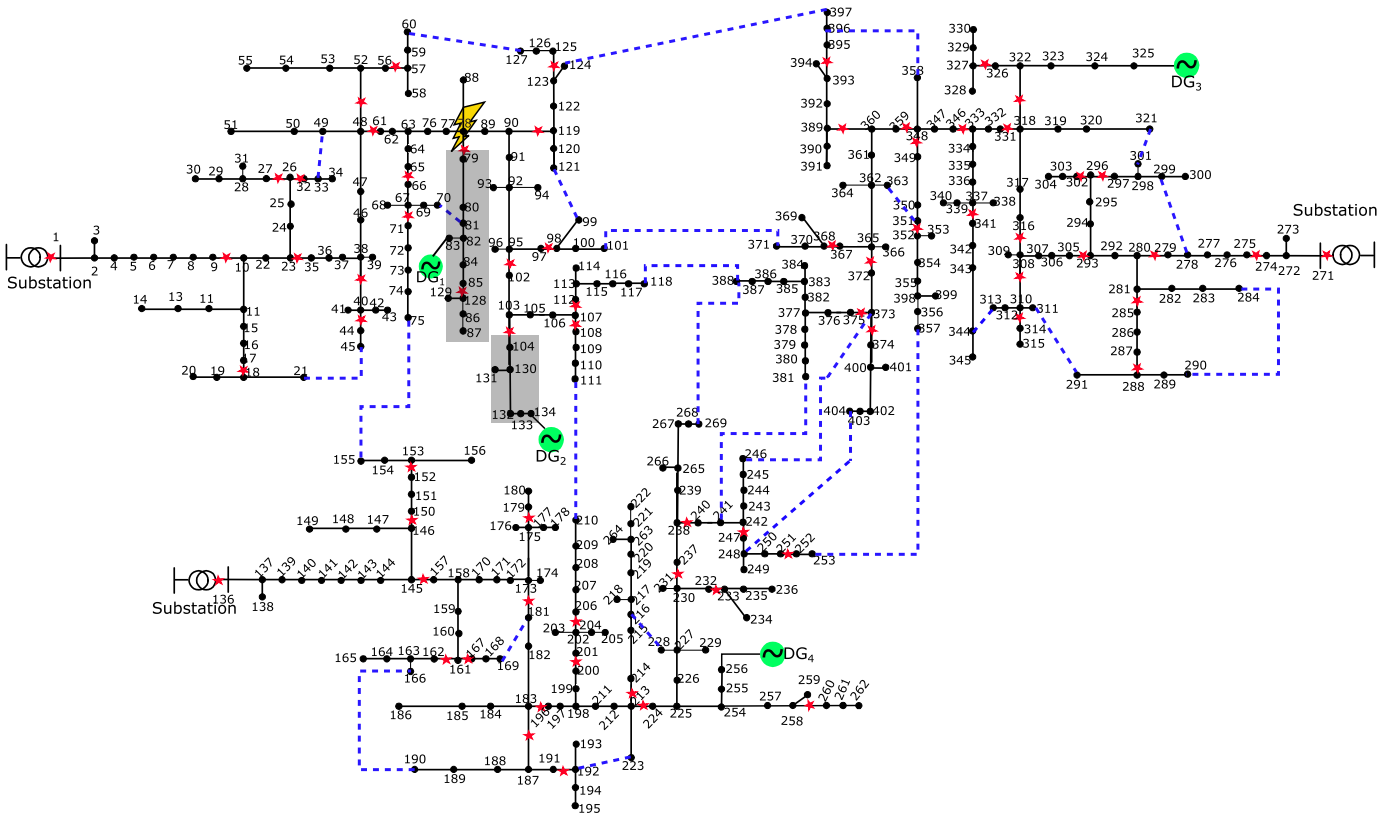


Fig. 4. Test system diagram (the stars represent NC remotely controlled switches, the blue dashed lines denote NO remotely controlled switches, the black circles represent load or passage buses and the black lines are electric conductors)

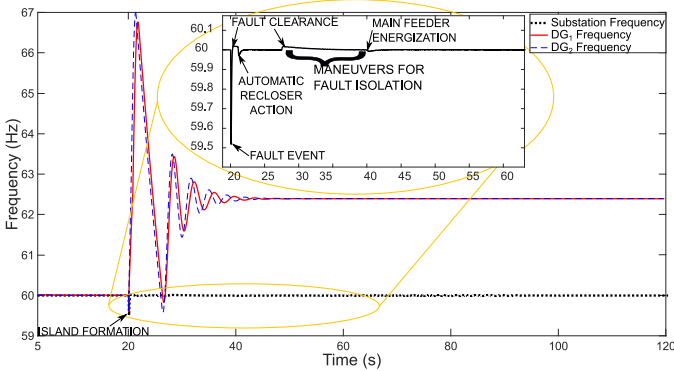


Fig. 5. Frequency behavior for scenario 1 - Load reconnection to the main feeder and transferring into islands without any frequency constraint

DGs in the DS is valid.

The most relevant information illustrated in Fig. 5 is the DGs' frequency rise after the islands' formation. Obviously, in the real world, such behavior would cause the protection system to operate, and the same occurs in our simulation: the frequency relays operate at 20.78 s and 20.51 s for DGs 1 and 2, respectively (more detail regarding the protective devices acting time can be found in [15]). The machines accelerate too much due to the sudden reduction of electrical torque, as the demands of the islands are far lower than the DGs' injections, causing an overfrequency scenario. Once the DGs' local protections operate, the steady-state frequency is given by (2) considering the island's demand equal to zero. As the machine's

mechanical torque is not set to zero once there local protection operates in this simulation, the steady-state frequency is not 60 Hz.

Additionally, we simulated in ATP-EMTP a second scenario wherein switches between buses 107-108 and 107-112 are initially open due to maintenance intervention and the rest of the system operates connected to the main feeder. Both switches are closed simultaneously, reconnecting the loads to the main grid, once the maintenance teams conclude the repairs, as illustrated in Fig. 6. This scenario can also represent the load reconnection, during SR process, to the neighboring feeders with GD. The frequencies fluctuations observed at both DGs (Fig. 6), caused by the demand variation (approximately 800 kW), are not enough to cause the generators' frequency protection action, since it is connected to the main grid. Thereby, it is possible to conclude that omitting frequency constraints from the SR optimization problem is valid if every power source is connected to the main grid.

C. SR with Steady-State Frequency Constraints

As demonstrated in the previous section, neglecting the power mismatches between the DG's pre-fault active power injection and the island's active demand may cause the protection system's action, in which case the island operation is not sustained. Adopting the frequency limits proposed in [5], assuming a 0.05 droop, and using (2), one can calculate that the DG's active setpoint must not differ from the AIR's active demand in more than 0.5 p.u. increment or 0.4 p.u. decrement. The AIR supplied by DG₁ has a 0.45 p.u. active demand, and DG₂ supplies an AIR demanding 0.26 p.u.. Therefore, in order to keep the DGs' frequencies within their local protection

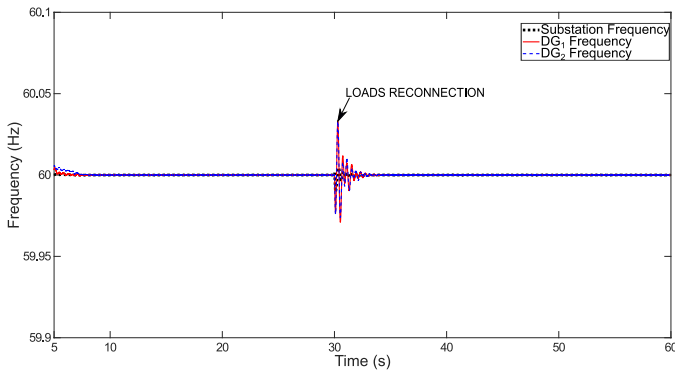


Fig. 6. Frequency behavior for scenario 2 - Load reconnection with DGs connected to the main feeder

thresholds, the DGs' active power injections should not surpass 0.85 p.u. and 0.66 p.u., respectively, at the moment of the islanding maneuver. The DGs' power production throughout the day do not necessarily meet the DISCO's needs. In this sense, there may be situations wherein the generator's power injection surpass the limits mentioned above; in these scenarios, the DGs' local protection would operate, shutting them off. Afterward, a black-start could take place, but this study is outside the scope of this paper. We address only the scenarios wherein the islands are automatically formed properly, *i.e.*, the DGs meet the proposed constraints when the fault strikes the DS. Adopting the DGs' new active setpoints as 0.8 p.u. and 0.6 p.u., respectively, and the same sequence of maneuvers presented in Table II, the frequency behavior at each DG is shown in Fig. 7.

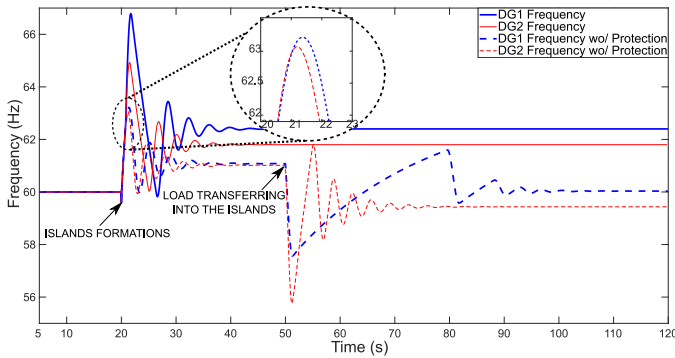


Fig. 7. Frequency behavior for scenario 3 - Load transferring into islands without dynamic constraints

The frequencies measured for both DGs are high enough to cause the frequency relays' operation. Note, however, that ignoring the trip signal, *i.e.*, considering a scenario without protective devices, the frequencies settle within the acceptable region (from 58.5 to 61.2 Hz) [5]. In this sense, one can conclude that by employing this constraint it is possible to determine whether or not the island's frequency in steady-state will cause the relays to operate in delayed action¹. However, the constraint is not sufficient to guarantee the island's maintenance, as it does not provide any information regarding the frequency's transient values.

As it can be observed in Fig. 7, there are some rapid frequency changes at $t=20s$ (measured using ATP's ideal frequency meters)

¹In accordance to IEEE Std. 1547, we adopt an 11 seconds delay for overfrequencies under 62 Hz and underfrequencies above 56.5 Hz.

that may not be perceived as promptly in a real scenario, since real frequency meters feeding the signals to the relays employ filters that delay and attenuate the frequency variation. In this sense, we present in Fig. 8 a more realistic frequency measure; in this case an averaging filter is applied to DG₁'s frequency signal observed in Fig. 7. The filter adopted in this example is a 10-cycle moving average. Note in the zoomed area that the frequency surpasses 62 Hz for more than a second, which is enough time to cause the relays operation even with the slow averaging filters. The same behavior is observed for every other study presented in this paper.

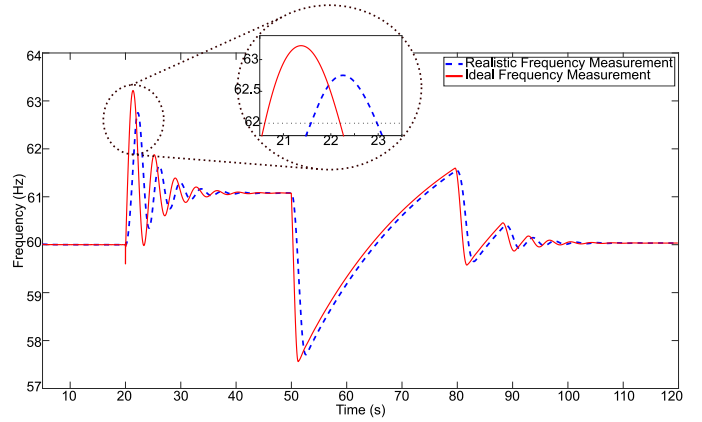


Fig. 8. Frequency behavior considering averaging filter

D. SR with Steady-State and Transient Frequency Constraints

The speed governor has some intrinsic delays such as the PID's integral term and the turbine model; hence, upon a sudden topology change, such as the island formation, the frequency is not controlled during the first seconds [12]. Instead, the accelerating power, which is related to the active power mismatch, is crucial in determining the frequency's critical value, which occurs during the transient's first seconds. For illustration, observe Fig. 7 wherein the active power mismatches between the DGs' pre-fault injections and the AIRs' demands are 0.35 p.u. and 0.34 p.u., respectively. It is noticeable that the transient frequency measured at DG₁ is slightly more severe than DG₂'s. Moreover, when a second load block is inserted into each island, the power mismatches are, respectively, -0.35 p.u. and -0.54 p.u., and, consequently, the critical frequency observed for DG₂ is much lower than for DG₁.

We carried out simulations in ATP-EMTP to verify the resulting transient critical frequency for several active power mismatch scenarios. We considered 5 setpoints and created active power mismatch situations to gather data regarding the relationship between the power mismatch and the critical frequency. The study consisted in placing the DGs in grid-connected mode injecting constant active power; suddenly, the DGs were switched to island operation in situations wherein the demand may not be the same as the power injection. These results were then compiled into a graph, shown in Fig. 9. The highlighted portion of the graph details the scenarios wherein the critical transient frequency is kept within the acceptable range, *i.e.*, there is neither overfrequency surpassing 62 Hz, nor underfrequency below 56.5 Hz.

Noteworthy, the highlighted portion is similar to first-degree equations; however, they are not equal as one would expect. The

justification for this is that we have modeled the system loads as impedances; therefore, the voltage at each load modifies its power demand. During the transient, the DGs' voltages are not constant and, as a consequence, neither are the islands' demands. In this sense, the power mismatches are not exactly the same in every simulation, thus the critical transient frequency deviation may also vary. Nonetheless, from Fig. 9 one can observe that as long as the active power mismatch is kept within the range $[-0.3, 0.2]$ p.u., the critical transient frequency should not cause the protective relays' fast operation, *i.e.*, in 0.16 sec as suggested in [5]. It is critical to highlight that although this range concerns the DGs and the controllers employed in this approach, the process can be repeated for any other DG.

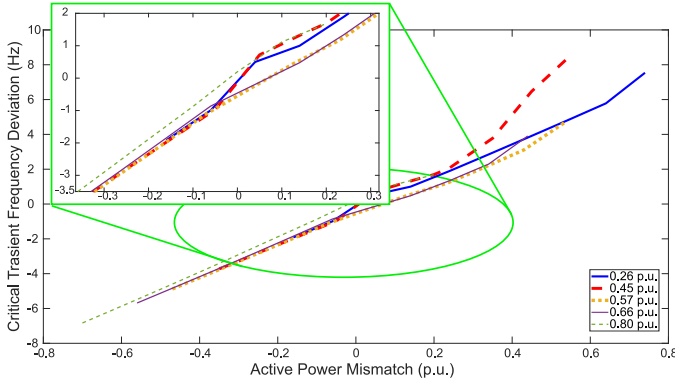


Fig. 9. Critical transient frequency deviation v.s. power mismatch

The sequence of maneuvers considering a fault at bus 78 is altered once we add the active power mismatch assessment as a constraint for every maneuver performed in the SR involving the islands, as exposed in Table III. Additionally, the DGs' prefault active power injection must not surpass the AIRs' demands in more than 0.2 p.u. in order to assure the island's maintenance. In this sense, the power injections of DGs 1 and 2 are set as 0.65 and 0.46 p.u., respectively. The frequency measurements at each DG node are illustrated in Fig. 10.

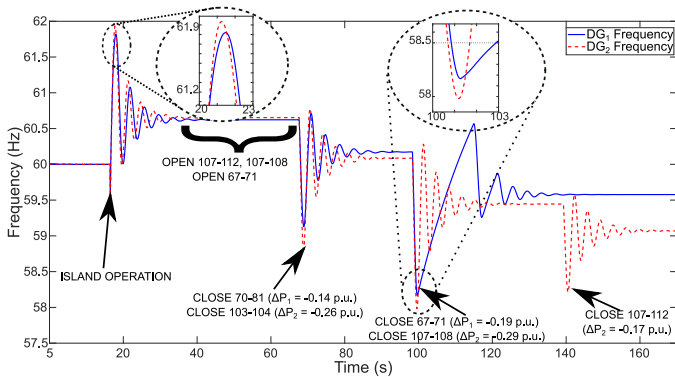


Fig. 10. Frequency behavior for scenario 4 - Load transferring into islands adopting dynamic constraints

The transient frequencies observed for both DGs at the beginning of their island operation are close to 62 Hz, but do not surpass the limit. This behavior was expected since the DGs' prefault power injections were set as the maximum possible values complying with the transient constraints. The power mismatches calculated for each

TABLE III
SEQUENCE OF MANEUVERS FOR SCENARIO 4

Scenario	Open*	Close*	ENS**	PNS***
	48-61	-		
	97-98	-		
	95-102	-		
	90-119	-		
	78-79	-		
	65-66	-		
	103-104	-		
	-	101-371		
Fault at Bus 78	107-112	-	269.57	0.00
	107-108	-		
	-	103-104		
	-	124-397		
	67-71	-		
	-	70-81		
	-	107-108		
	-	67-71		
	-	107-112		

* Switches between buses.

** Value in kWh calculated for the final topology disregarding the ENS of the faulted sector.

*** (PNS = Power Not Supplied) Value in kW calculated for the final topology disregarding the PNS of the faulted sector.

maneuver that adds a load block into the islands, in general, are not close to -0.3 p.u., which justifies the relatively mild transient frequencies after the maneuvers. The maximum and minimum feasible loading of each DG is determined by the steady-state constraints (4). In this scenario and disregarding the AGC's action, DG₁ can supply an island with demand ranging from 15% to 100% of its capacity (assuming that the DG's minimum injection is lower than 0.15 p.u.); for DG₂ the isolated region (island) demand's lower limit is DG's minimum power and the upper limit is 96% of the DG's capacity. Once the AGC operation modifies the DGs' active setpoints, every generator may inject its full capacity into an island.

Noteworthy, there may be situations during the DS operation wherein the active setpoints of DGs are not close to their islands demands for any number of reasons. In such scenarios, the generators' local protection would actuate, shutting them off. Considering a disaster situation wherein there are no maneuvers to reconnect the loads to the substation nor transfer them to another feeder, a manual (rather than automatic) island operation may be of service [11]. Assuming that the DGs are capable of performing black-start and are compensated for it, the constraints presented in this section can also be employed to determine how the load blocks should be inserted into the island depending on the machine's setpoint and instantaneous active power injection.

V. CONCLUSION

In this paper we propose modifications to the classic SR problem by adding new constraints that ensure the maintenance of DGs operating in island mode throughout the transients caused by switching maneuvers during contingencies. We add two types of constraints into the optimization model for each DG to ensure the maintenance of their island operation: one to establish the island's minimum and maximum demand, and another to ensure that the maneuvers involving an islanded DG do not cause the generator's local protection to operate. We employ a MOEA to solve the SR problem and then we validate the feasibility of the SRP in ATP-EMTP environment. The speed governor and exciter of each

DG, as well as the DS's protective system (relays, IIDs, automatic reclosers and fuses), are also modeled in ATP-EMTP.

We tested the proposed model on a 3-feeder 405-bus system to analyse the transient behavior of two DGs, modeled as synchronous machines moved by steam turbines. The simulations in ATP-EMTP confirm the feasibility of the solutions obtained considering the proposed augmented optimization model (composed of the proposal found in [9] and the novel constraints proposed in this paper). In this sense, we have successfully converted the critical information regarding the transient frequency deviation into static constraints. Thus, we can apply the MOEA proposed in [9] for solving the modified SR problem, instead of simulating the DGs' behavior for every attempt to add or remove loads from the island, which would be time-consuming.

Further research may address: (1) the employment of other types of generators, speed governors and different primary sources, which would modify the frequency's transient behavior; (2) the investigation of transient constraints aiming to relate frequency behavior, power mismatch, and both physical and controlling parameters mathematically; (3) adding the loads' transient behaviors when they are re-supplied via island operation into the model (*e.g.* cold and warm load pickup, transformer magnetization and motor starts), as these events may lead to protection misoperations; and, (4) enhancing the frequency meter model to represent better the relay's real operation.

REFERENCES

- [1] A. R. Vieira, V. S. Batista, G. C. Júnior, and J. P. A. Vieira, "Integrating protection constraints to a mean-based method for service restoration in radial distribution systems," *Electric Power Systems Research*, vol. 191, pp. 1–15.
- [2] M. H. Camillo, R. Z. Fanucchi, M. E. Romero, T. W. de Lima, A. da Silva Soares, A. C. B. Delbem, L. T. Marques, C. D. Maciel, and J. B. A. London Jr., "Combining exhaustive search and multi-objective evolutionary algorithm for service restoration in large-scale distribution systems," *Electric Power Systems Research*, vol. 134, pp. 1–8, 2016.
- [3] L. T. Marques, A. C. B. Delbem, and J. B. A. London Jr., "Service restoration with prioritization of customers and switches and determination of switching sequence," *IEEE Transactions on Smart Grid*, vol. 9, no. 3, pp. 2359–2370, May 2018.
- [4] A. Stankovic, "The definition and quantification of resilience," IEEE PES Industry Technical Support Task Force, Tech. Rep., 2018.
- [5] "IEEE Standard for Interconnection and Interoperability of Distributed Energy Resources with Associated Electric Power Systems Interfaces," *IEEE Std 1547-2018 (Revision of IEEE Std 1547-2003)*, pp. 1–138, 2018.
- [6] K. P. Schneider, F. K. Tuffner, M. A. Elizondo, C.-C. Liu, Y. Xu, and D. Ton, "Evaluating the feasibility to use microgrids as a resiliency resource," *IEEE Transactions on Smart Grid*, vol. 8, no. 2, pp. 687–696, 2016.
- [7] F. Shen, Q. Wu, and Y. Xue, "Review of service restoration for distribution networks," *Journal of Modern Power Systems and Clean Energy*, vol. 8, no. 1, pp. 1–14, 2020.
- [8] R. A. V. Peralta, J. B. Leite, and J. R. S. Mantovani, "Automatic restoration of large-scale distribution networks with distributed generators, voltage control devices and heating loads," *Electric Power Systems Research*, vol. 176, no. 105925, 2019.
- [9] E. O. P. Carvalho, J. P. R. Fernandes, L. T. Marques, and J. B. A. London Jr., "Multi-Objective Evolutionary Algorithm for Service Restoration in the Presence of Distributed Generation," in *2020 Simpósio Brasileiro de Sistemas Elétricos*, 2020.
- [10] W. R. Faria, M. Oleskovicz, D. V. Coury, R. B. Otto, and B. R. Pereira, "Intentional island and dynamic analysis of a microgrid," in *2019 IEEE Milan PowerTech*, 2019, pp. 1–6.
- [11] Y. Xu, C.-C. Liu, K. P. Schneider, F. K. Tuffner, and D. T. Ton, "Microgrids for service restoration to critical load in a resilient distribution system," *IEEE Transactions on Smart Grid*, vol. 9, no. 1, pp. 426–437, 2016.
- [12] P. Pourbeik, G. Chown, J. Feltes, F. Modau, S. Sterpu, R. Boyer, K. Chan, L. Hannett, D. Leonard, L. Lima, W. Hofbauer, L. Gerin-Lajoie, S. Patterson, J. Undrill, and F. Langenbacher, "Dynamic models for turbine-governors in power system studies," Power System Dynamic Performance Committee, Tech. Rep., 2013.
- [13] "IEEE Recommended Practice for Excitation System Models for Power System Stability Studies," *IEEE Std 421.5-2016 (Revision of IEEE Std 421.5-2005)*, pp. 1–207, 2016.
- [14] K. Pereira, B. R. Pereira, J. Contreras, and J. R. S. Mantovani, "A multi-objective optimization technique to develop protection systems of distribution networks with distributed generation," *IEEE Transactions on Power Systems*, vol. 33, no. 6, pp. 7064–7075, 2018.
- [15] W. R. Faria, E. O. P. Carvalho, L. B. Dantas, C. D. Maciel, J. B. A. London Jr., and B. R. Pereira Jr., "Dataset for Service Restoration Studies in a Power Distribution System Addressing the Transient Behavior of Synchronous Machines," Mar. 2021. [Online]. Available: <https://doi.org/10.5281/zenodo.4603896>